Lab in a tube: a fast-assembled colorimetric sensor for highly sensitive detection of oligonucleotides based on hybridization chain reaction

Siqi Zhang [a], Kun Wang [b], Zhenyu Li [a], Zhongmin Feng [a], Ting Sun [a*]

[a] College of Sciences, Northeastern University, Shenyang, 110819, China

[b] Department of Chemistry and Environmental Engineering, Changchun University of Science and Technology, Changchun, China

*Corresponding author

E-mail: sun1th@163.com

Tel.: +86-024-83684786;

Second structure of H_1 and H_2

As shown in Figure S6 (supporting information), the CD spectra of hairpin H_1 and H_1 contains a positive long wavelength band or bands at about 260–280nm and a negative band around 245 nm. According to the previous report[1], the hairpins are the B-form DNA.

The mechanism of yellow color development

3,5,3',5'-Tetramethylbenzidine is a common chromogenic substrate of peroxidase enzymes such as horseradish peroxidase. Its one- or two-electron oxidation develops a blue- or yellow-colored product, respectively[2]. The sequences of reactions that seem to be involved in the colorimetric T_{HBV} determination technique are summarized below:

$H_2O_2 \xrightarrow{\text{horseradish peroxidase}} 2OH \bullet$

$2OH \bullet$ +TMB(colorless λ=285 nm) $\xrightarrow{\text{horseradish peroxidase}}$ H_2O+ one-electron oxidation TMB(blue, λ=370 nm and 652 nm)

oxidation TMB(blue)+ $2OH \bullet$ $\xrightarrow{HCl}$ two-electron oxidation TMB(yellow λ=452 nm)+ H_2O

As shown in scheme 1, the system can form G-quadruplex upon addition of T_{HBV}. G-quadruplexes can bind hemin to form a kind of DNAzyme which will mimic catalytic activity like horseradish peroxidase (HRP) in the presence of K^+. It has been proven that in the presence of the DNAzymes, H_2O_2-mediated oxidation of TMB could be sharply speeded up compared to the conditions without DNAzymes. In visible region, no peak for TMB was appeared initially, so the TMB was colorless. While H_2O_2 gradually oxidized TMB, two new peaks appear, at 370 and 652 nm. The compounds appear blue. Upon addition of 1M HCl, one- electron oxidation TMB was transformed into two- electron oxidation TMB and these peaks were replaced by a peak at 452 nm.

Optimization of the experimental parameters

As shown in Figure S3, raising the temperature will contribute to speed up the DNA self-assembly efficiently. The rate of rise for the DNA self-assembly slows gradually when experiment was conducted above 25℃. In consideration of convenience of experimental operation, the 25℃ (room temperature) was chosen as the reaction temperature.

Other experimental parameters (e.g. pH value, K^+ concentration, and Mg^{2+} concentration) that effect the self-assembly of the colorimetric biosensor were optimized and exhibited in Figure S8. The effect of the absorbance to pH value ranging from 5 to 9 was investigated. As shown in Figure S8A, the absorbance showed no obvious undulation at different pH values. In order to simplify working processes, 8 was chosen as the reasonable pH value. Other experimental parameters which need to optimized are K^+ and Mg^{2+} concentration. The effect of the absorbance to K^+ concentration ranging from 0 mM to 25 mM was investigated. Since K^+ can help the G-quadruplex form a stable hemin/G-quadruplex structure, increasing K^+ concentration is favorable to accelerate the DNA self-assembly. As shown in Figure S8B, the absorbance gradually increased until adding 15 mM K^+. Then a further increase of K^+ concentration could not make the absorbance rise. Thus 15 mM was chosen as the reasonable K^+ concentration. And the effect of the absorbance to Mg^{2+} concentration ranging from 0 mM to 10 mM was also investigated. As shown in Figure S8C, the absorbance rose slowly with the Mg^{2+} concentration increasing. According to this result, we selected 5 mM Mg^{2+} concentration in the throughout experiment.

Array detection for target DNA using multiple of 96 samples

We also develop a low-cost oligonucleotides analysis platform for target DNA using multiple of 96 samples. We select numerous mutations at different positions of target sequence, such as single base mismatches in segment A of target DNA, ($T1_{AA}$, T_{1AC}, T_{1AG}), in segment B (T_{1B}) and in segment C (T_{1C}) of target DNA, two-base

mismatches located in different segments of target DNA, (T_{2AB}, T_{2AC}, T_{2BC}) and a three-base mismatch (T_3). The detailed sequence of the oligonucleotide is listed as follows:

T_{HBV}: 5'-AGTTACTC TCTTTTTTG CCTTCTGA-3'

T_{1AG}: 5'-AGTTACTC TCTTTTTTG GCTTCTGA-3'

T_{1AA}: 5'-AGTTACTC TCTTTTTTG ACTTCTGA-3'

T_{1AT}: 5'-AGTTACTC TCTTTTTTG TCTTCTGA-3'

T_{1B}: 5-AGTTACTC TCTTATTTG CCTTCTGA-3

T_{1C}: 5-AGTTACTT TCTTTTTTG CCTTCTGA-3

T_{2AB}: 5-AGTTACTC TCTTATTTG ACTTCTGA-3

T_{2BC}: 5-AGTTACTT TCTTATTTG CCTTCTGA-3

T_3: 5-AGTTACTT TCTTATTTG ACTTCTGA-3

Each mutation was prepared in different concentrations (0 nM, 0.1 nM, 1 nM, 10 nM, 30 nM, 50 nM, 70 nM, 100 nM). The analysis experiment was conducted in a multiple of 96 samples. As shown in Figure S9, the target DNA of the proper concentration can be recognized just by bare eye. So we believe our method has potential for high-throughput screening.

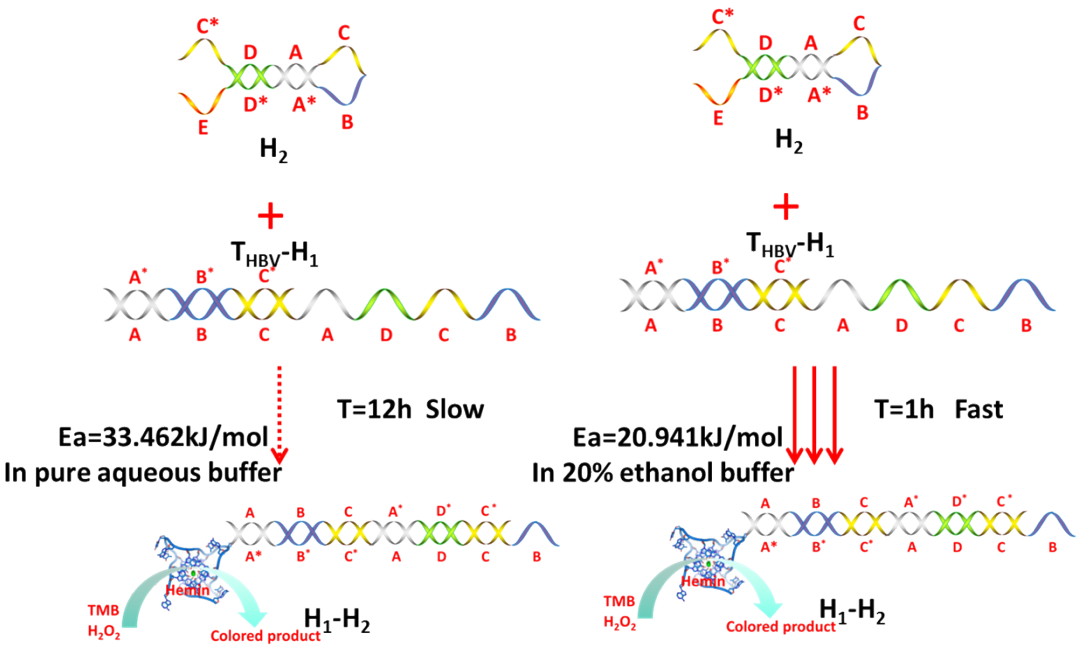

1

2 Fig. S1 (a) hybridization chain reaction in buffer solution and 20% ethanol solution.

3

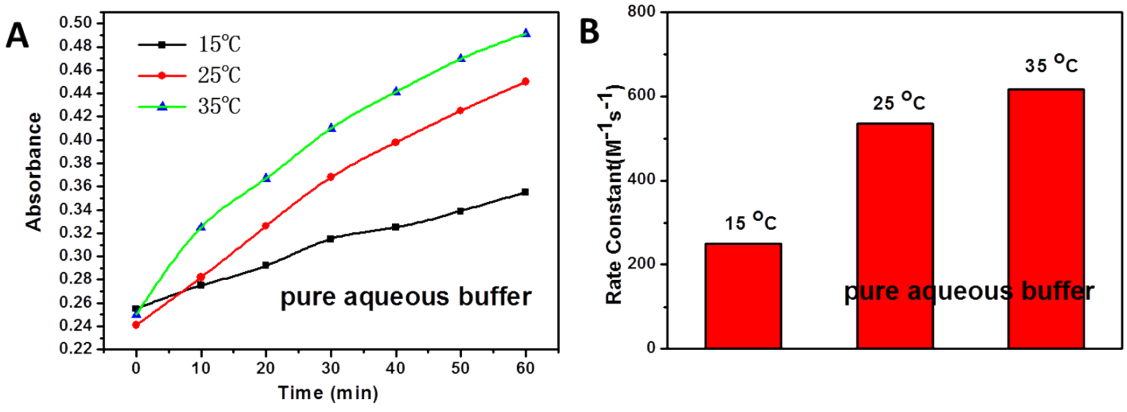

4

5 Fig. S2 (A) UV-vis absorbance of the hybridization chain reaction for system at

6 different temperatures in pure aqueous buffer in 60 min. (B) The rate constant of the

7 hybridization chain reaction for system at different temperatures in pure aqueous

8 buffer after 1 h. [H_1]=100 nM, [H_2]=100 nM, [T_{HBV}]=50 nM.

9

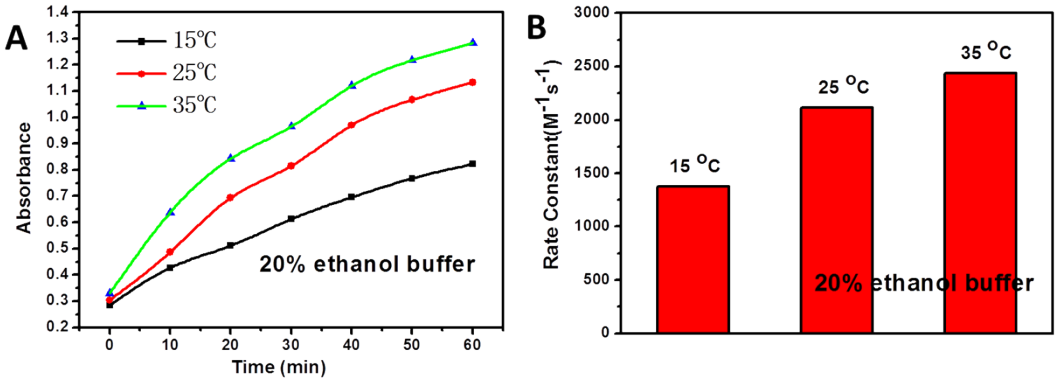

Fig. S3 (A) UV-vis absorbance of the hybridization chain reaction for system at different temperatures in 20% ethanol buffer in 60 min. (B) The rate constant of the hybridization chain reaction for system at different temperatures in 20% ethanol buffer after 1 h. $[H_1]$=100 nM, $[H_2]$=100 nM, $[T_{HBV}]$=50 nM.

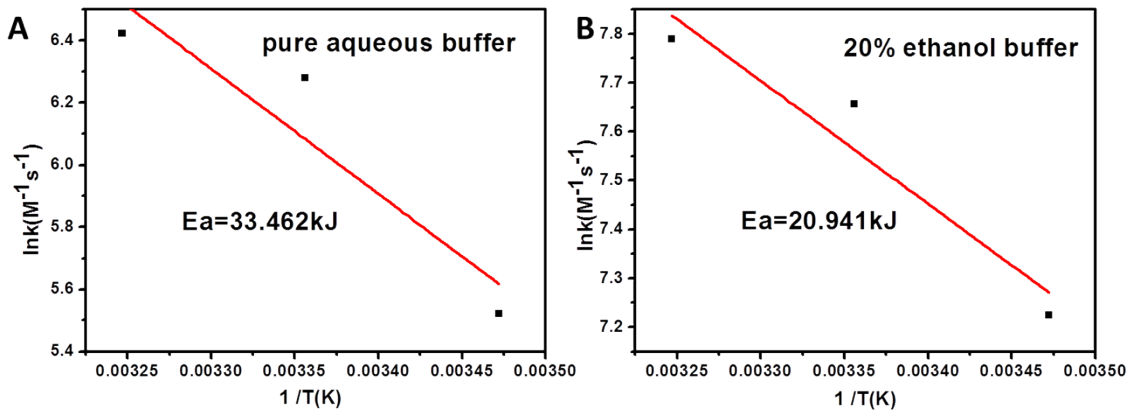

Fig. S4 (A) Arrhenius plots for the strand exchange reaction in pure aqueous buffer. (B) Arrhenius plots for strand exchange reaction in 20% ethanol buffer. Values of activation energies (Ea) were calculated from the Arrhenius plots.

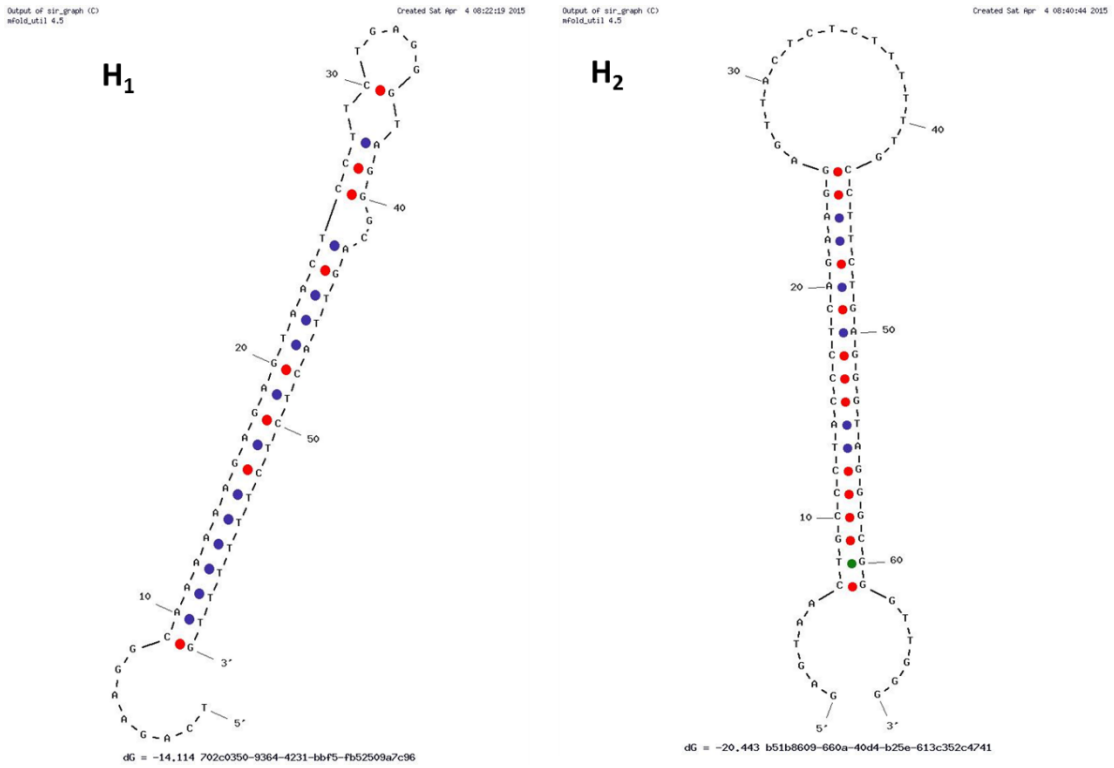

Fig. S5 Second structure of H_1 and H_2. H_1: ΔG=-20.44 kcal.mole^{-1}, Tm=72.1℃, ΔH=-149.9 kcal.mole^{-1}, ΔS= -434.21 cal.K^{-1}mole^{-1} H_2: ΔG=-20.44 kcal.mole^{-1}, Tm=72.1℃, ΔH=-149.9 kcal.mole^{-1}, ΔS= -434.21 cal.K^{-1}mole^{-1}

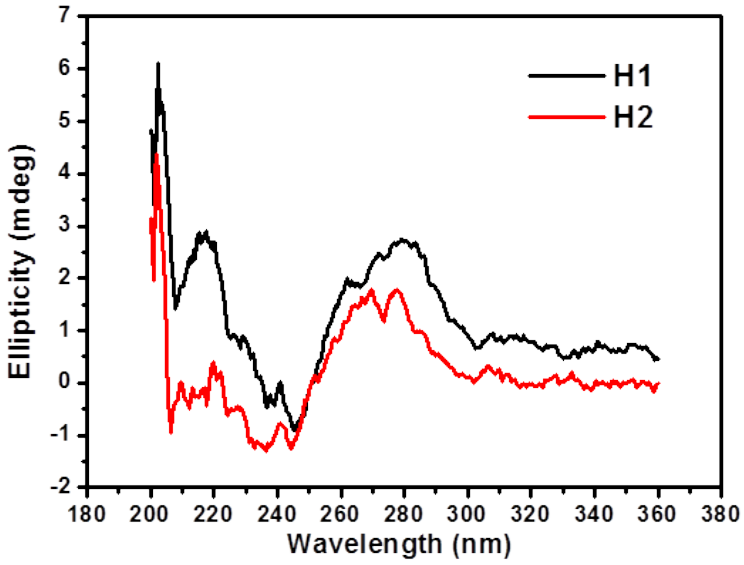

Fig. S6 CD spectra of H_1 and H_2. The concentrations of H_1 and H_2 were 1 μM.

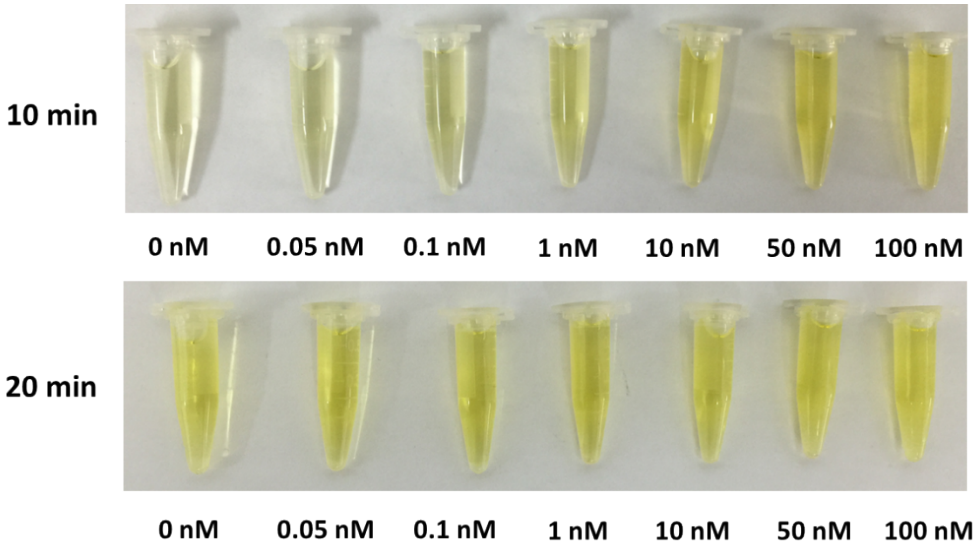

Fig. S7 Effect of TMB−H_2O_2 reaction time on the DNAzyme activity

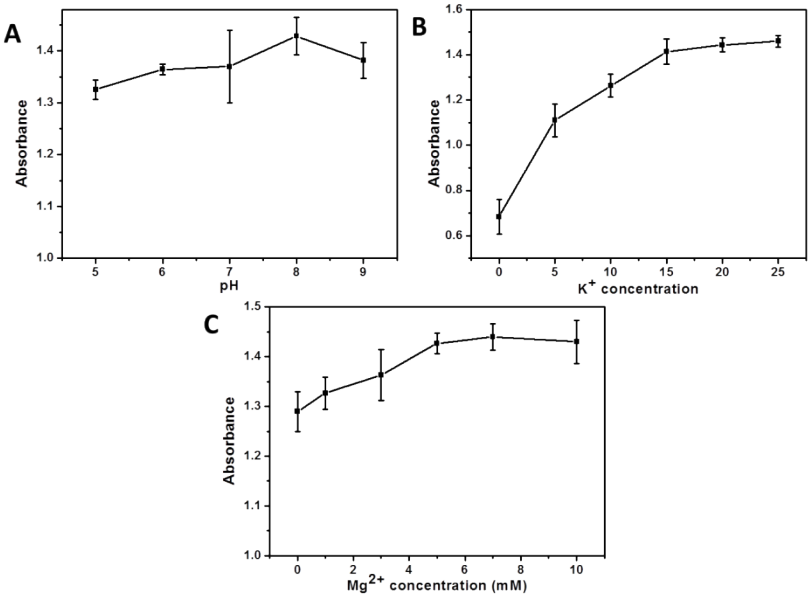

Fig. S8. Effect of (A) pH, (B) K^+ concentration, (C) Mg^{2+} concentration in process of hybridization chain reaction on the absorbance at 452 nm was investigated. The error bars represent the standard deviation of three independent measurements. [H_1]=100 nM, [H_2]=100 nM, [T_{HBV}]=50 nM.

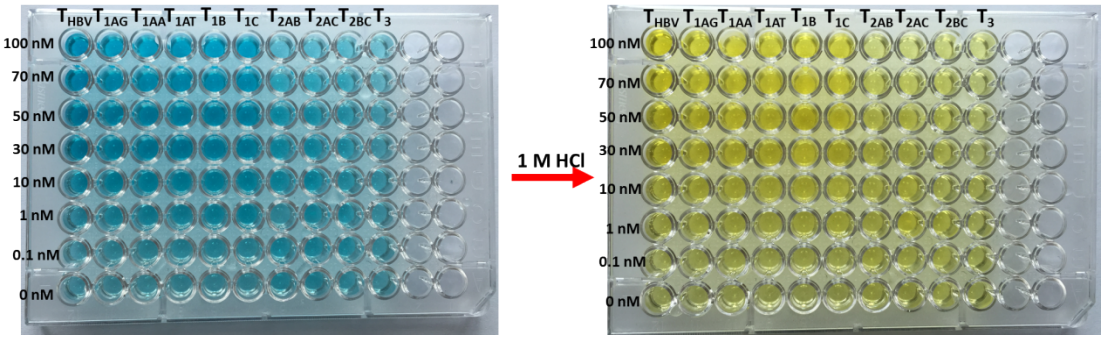

Fig. S9 Array detection for target DNA using multiple of 96 samples. (A) Photo images of the solution color change with different concentration mutants of the analyte. (B) Photo images of the solution color change with different concentration mutants of the analyte after adding 1 M HCl. $[H_1]$=100 nM, $[H_2]$=100 nM, $[T_{HBV}]$=50 nM.

1. J. Kypr, I. Kejnovska, D. Renciuk and M. Vorlickova, *Nucleic Acids Research*, 2009, 37, 1713-1725.
2. N. A. Bagirova, T. N. Shekhovtsova and R. B. van Huystee, *Talanta*, 2001, 55, 1151-1164.